Case Studies in Thermal Engineering 30 (2022) 101721

Contents lists available at ScienceDirect

Case Studies in Thermal Engineering

journal homepage: www.elsevier.com/locate/csite

Air-side performance of embedded and welded spiral fin and tube heat exchangers

Parinya Kiatpachai [a,b], Thawatchai Kaewkamrop [b], Mehrdad Mesgarpour [b], Ho Seon Ahn [c], Ahmet Selim Dalkılıç [d], Omid Mahian [e,f], Somchai Wongwises [b,g,*]

[a] Department of Mechanical Engineering, Academic Division, Chulachomklao Royal Military Academy, Nakhon, Nayok, 26001, Thailand
[b] Fluid Mechanics, Thermal Engineering and Multiphase Flow Research Lab (FUTURE), Department of Mechanical Engineering, King Mongkut's University of Technology Thonburi (KMUTT), Bangmod, Bangkok, 10140, Thailand
[c] Department of Mechanical Engineering, Incheon National University, Incheon, Republic of Korea
[d] Department of Mechanical Engineering, Yildiz Technical University, Yildiz, Besiktas, Istanbul, Turkey
[e] School of Chemical Engineering and Technology, Xi'an Jiaotong University, Xi'an, China
[f] Department of Mechanical Engineering, Center for Nanotechnology in Renewable Energies, Ferdowsi University of Mashhad, Mashhad, Iran
[g] National Science and Technology Development Agency (NSTDA), Pathum Thani, 12120, Thailand

ARTICLE INFO

Keywords:
Heat transfer
Energy
Finned tube
Heat exchanger
Spiral fin-and-tube heat exchangers

ABSTRACT

This paper presents the air-side performance (ASP) of embedded and welded spiral fin and tube heat exchangers (SFTHXs). Six heat exchangers were tested to investigate the effects of fin-base connections and fin pitch. Test sections were fabricated from steel tubes, with two rows of tubing and a Z-shaped water flow arrangement, and an aluminum fin with various fin pitches. The experiment was done at a high Reynolds number of air flow (4000–18000). The results show that fin pitch had no effect on the ASP of embedded SFTHXs. In contrast, fin pitch influenced the ASP of the welded SFTHX. Moreover, the pressure drop decreased with increasing fin pitch, whereas the friction factor was lower for a smaller fin pitch. Due to better fin base connections, an embedded spiral fin generally provided a higher heat transfer rate than a welded spiral fin did. The pressure drop of the welded spiral fin was greater than that of the embedded spiral fin, possibly because the welded spiral fin had melted slag at the fin base.

Nomenclature

A_{min}	Minimum free flow area, m^2
A_p	Cross-sectional or profile area of fin, m^2
c_p	Specific heat at constant pressure, J/(kg.K)
k	Thermal conductivity, W/(m.K)
Pr	Prandtl number
r_i	Fin base radius, m
r_o	Fin tip radius, m
R	Radius function

* Corresponding author. Fluid Mechanics, Thermal Engineering and Multiphase Flow Research Lab (FUTURE), Department of Mechanical Engineering, King Mongkut's University of Technology Thonburi (KMUTT), Bangmod, Bangkok, 10140, Thailand.
E-mail address: somchai.won@kmutt.ac.th (S. Wongwises).

https://doi.org/10.1016/j.csite.2021.101721
Received 7 October 2021; Received in revised form 10 December 2021; Accepted 17 December 2021
Available online 18 December 2021

Greek symbols

η_o	Overall surface effectiveness
ρ	Density, kg/m^3
σ	Contraction ratio of cross-sectional area
φ	Combination of terms
ψ	Radius ratio

Subscripts

1	Air inlet
2	Air outlet
a	Air
em	Embedded spiral fin
i	Tube-side
in	Inlet
m	Mean value
max	Maximum
t	Tube
w	Water
weld	Welded spiral fin

1. Introduction

Spiral fin and tube heat exchangers (SFTHXs) can be used for cooling and heating systems. Depending on the main objective, an application system is usually required. Pongsoi et al. [1] concentrated on and reviewed (until 2014) the air-side performance (ASP) of SFTHXs. They suggested that the SFTHX was a favored type of thermal equipment for energy saving and emission reduction policies in industrial applications. Furthermore, they analyzed the effect characteristics of inside tube diameter (d_i), outside fin diameter (d_f), fin thickness (f_t), fin pitch (f_p), number of tube rows (N_{row}), longitudinal tube pitch (P_L), transverse tube pitch (P_T), tube arrangement, fin material, fin pattern, fin alignment, operating conditions, and so forth on the ASP of SFTHXs. Furthermore, the SFTHX design has caused developments in fin and tube heat exchangers, as well as other heat exchangers.

During 2011–2020, the research group [2–14] presented evidence of ASPs for crimped, L-footed, conventional, serrated, wired, and multiple SFTHXs. For the crimped spiral fin [2–5] and L-footed spiral fin [6,7], they studied the effect of fin material, N_{row}, f_p, and small d_i on the ASP of SFTHX. The experimental results showed that fin material, f_p, and N_{row} had significant effects on ASP. For the conventional spiral fin, Ramesh et al. [8] tested the conventional SFTHX for an air-cooled spiral radiator and reported the performance in terms of h_o, log mean temperature difference (*LMTD*), heat exchanger effectiveness (ε), and Nusselt number (*Nu*). Moreover, Unger et al. [9] studied the free convection heat transfer for conventional SFTHXs at tilt angles of 0°, 20°, 30°, and 40° and found that the tilt angles had significant effects on the ASP of conventional SFTHXs. Pongsoi et al. [10] examined the effect of f_p on the ASP of SFTHXs and proposed a correlation of serrated SFTHX for designing the total surface area (A_o) of the heat exchanger (HX). In addition, Zhaou et al. [11] compared the ASPs obtained from twisted-serrated SFTHXs and serrated SFTHXs and confirmed that the twisted serrated SFTHX had better h_o than the serrated SFTHX did. Youssef et al. [12] developed the wired SFTHX for experiment and simulation, using CFD to predict the phase-change material process in latent heat storage applications. For multiple fins, Kumar et al. [13] studied the effect of fin patterns on the ASP of crimped and serrated SFTHXs and compared them with plain and circular FTHXs using 3D CFD simulations. They found that a spiral fin had a higher Colburn factor (j) and friction factor (f) than plain and circular fins did. In addition, the turbulent flow with vortices generation was analyzed to learn and understand the flow characteristics. Bosnjakovic et al. [14] compared a star-shaped SFTHX and a conventional SFTHX. The results showed that the Nusselt number, fin efficiency (η_f), heat flux, and heat transfer rate (Q) of star-shaped SFTHXs were greater than those of conventional SFTHXs with an outside tube diameter (Re_{do}) Reynolds number range from 2,000 to 13,000. The spiral-finned tube shape has also been applied to innovative shell and tube heat exchangers and spirally finned pin heat exchangers, as proposed in Naqvi et al. [15] and Chang et al. [16].

Over the years, studies about SFTHXs have concentrated on the ASPs of crimped, L-footed, conventional, serrated, star-shaped, and wired spiral fins. Embedded and welded SFTHXs are alternatives for practical applications due to the higher strength of the fin base connection when compared with other fin types. Despite its importance, the relationship between fin base connection and fin pitch with the ASP of SFTHXs remains unstudied. In the present study, the main concern is the effect of fin base connection and fin pitch on the heat transfer and pressure drop characteristics at high Reynolds numbers for SFTHXs. Moreover, correlations for the j factor

Table 1
Geometrical details of the heat exchangers.

Spiral fin types	d_i (*mm*)	d_o (*mm*)	d_f (*mm*)	P_L (*mm*)	P_T (*mm*)	f_t (*mm*)	n_t	N_{row}	Fin materials	f_p (*mm*)
Embedded	21.2	25.4	51.4	68.5	66	0.5	5	2	*Al*	***2.5, 3.2, and 4.2***
Welded	21.2	25.4	51.4	68.5	66	0.5	5	2	*Al*	***2.5, 3.2, and 4.2***

Note: Tube and fin materials are iron (Fe) and Aluminum (Al), respectively. The n_t represents the number of tubes in row.

(Colburn factor) and f factor (friction factor) are proposed for industrial applications.

2. Data reduction

The present study used the apparatus described by Pongsoi et al. [2]. Table 1 shows the geometric details of embedded and welded SFTHXs. An aluminum fin and a steel tube were assembled for the test sections. Table 2 shows the experimental conditions. Fig. 1 illustrates the schematic diagrams for both SFTHXs and the water flow arrangement. The overall heat transfer coefficient (U) is calculated using

$$\frac{1}{UA}=\frac{1}{h_iA_i}+\frac{\ln(d_o/d_i)}{2\pi k_tL}+\frac{1}{\eta_o h_o A_o} \tag{1}$$

Based on the multipass parallel cross flow (MPC) and multipass counter cross flow (MCC), the heat exchanger effectiveness (ε) and the number of transfer units (NTU) can be calculated from the following.

For MPC with $N_{row} = 2$:

$$\varepsilon_p=\left(1-\frac{K}{2}\right)\left(1-e^{-2K/C_A^*}\right)\ ,K=1-e^{-NTU_A\left(C_A^*/2\right)} \tag{2}$$

For MCC with $N_{row} = 2$:

$$\varepsilon_c=1-\left[\frac{K}{2}+\left(1-\frac{K}{2}\right)e^{2K/C_A^*}\right]^{-1},K=1-e^{-NTU_A\left(C_A^*/2\right)} \tag{3}$$

where C_c/C_h or C_h/C_c represents $C^* = C_{min}/C_{max}$, which is the heat capacity rate ratio obtained from cold fluid and hot fluid. The combination of both flow configurations is used to determine the average effectiveness.

$$\varepsilon_{pc}=\frac{\varepsilon_p+\varepsilon_c}{2}\ \text{for}\ N_{row}\ =\ 2. \tag{4}$$

The radial fin efficiency, in terms of Gardner's [17] modified Bessel functions, is used for data reduction.

$$\eta_f=\frac{2\psi}{\varphi(1+\psi)}\frac{I_1(\varphi R_o)K_1(\varphi R_i)-I_1(\varphi R_i)K_1(\varphi R_o)}{I_0(\varphi R_i)K_1(\varphi R_o)+I_1(\varphi R_o)K_0(\varphi R_i)} \tag{5}$$

where

$$\varphi=(r_o-r_i)^{3/2}\left(\frac{2h_o}{k_fA_p}\right)^{1/2} \tag{6}$$

The air-side heat transfer performance is evaluated based on the j factor.

$$j=\frac{Nu}{\mathrm{Re}_{do}\mathrm{Pr}^{1/3}}=\frac{h_o}{\rho_aV_{\max}c_P}(\mathrm{Pr})^{2/3} \tag{7}$$

The ΔP across the HX is shown as friction factor [18].

$$f=\left(\frac{A_{\min}}{A_o}\right)\left(\frac{\rho_m}{\rho_1}\right)\left[\frac{2\Delta P\rho_1}{G_c^2}-\left(1+\sigma^2\right)\left(\frac{\rho_1}{\rho_2}-1\right)\right] \tag{8}$$

The ANSI/ASHRAE's 33 standards [19] (i.e., $|Q_a - Q_w|/Q_{ave} < 0.05$) are used to check the complete energy balance between both working fluids across the test sections. For the uncertainty analysis, the root mean sum square method was used for calculating the uncertainty. The j and f factors have maximum uncertainties of 5.37% and 6.61%, respectively. These maximum uncertainties were the values at the lowest Reynolds number. The uncertainties of the j and f factors increased as the Reynolds number decreased. These uncertainties were taken into account when investigating the ASP.

3. Results and discussion

This study focused on the effect of fin base connection and f_p on the ASPs of embedded and welded SFTHXs. The test sections with a f_p of 2.5–4.2 mm were investigated at high Re_{do}. The heat transfer rate between air and water under sensible heating was investigated. The tube-side hot water flow is a Z-shaped flow arrangement, that provides good distribution of fluid flow.

Table 2
Experimental conditions.

$T_{a,in}$, ^oC	31.5 ± 0.5
V_{fr}, m/s	2-8 or Re_{do} (4,000–18,000)
$T_{w,in}$, ^oC	55–65
m_w, kg/s	0.167–0.233

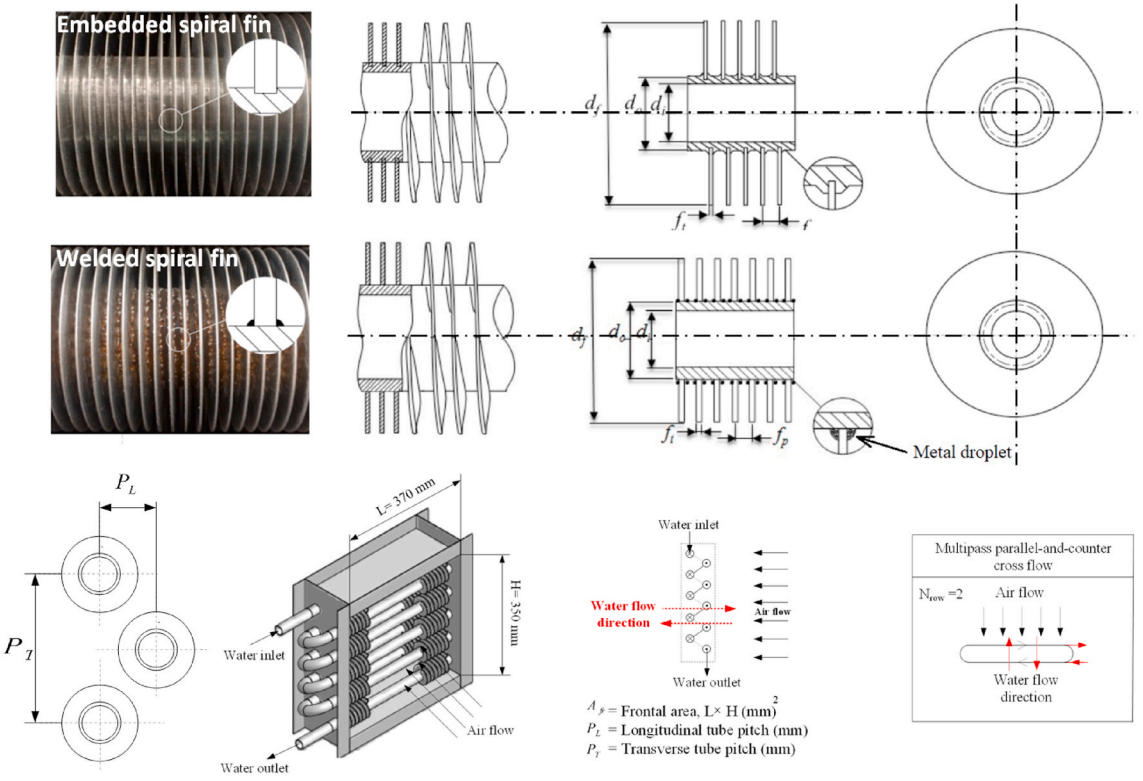

Fig. 1. Photos and schematic of the tested embedded and welded SFTHXs and flow arrangement.

Fig. 2 demonstrates the experimental data at $T_{w,in} = 60$ °C and $m_{w,in} = 0.2$ kg/s. The air-side heat transfer coefficient (h_o), pressure drop (ΔP), and average heat transfer rate (Q_{ave}) are clarified for the ASP analysis. As shown, Q_{ave}, h_o, and ΔP increase with increasing frontal air velocity (V_{fr}). Fig. 2(a) shows that the Q_{ave} increases as the f_p decreases for both fin types. For the embedded SFTHX, the f_p has a significant effect on Q_{ave} because of the increase in the A_o when f_p is reduced from 4.2 to 2.4 mm. However, for welded SFTHXs, the Q_{ave} trend at various f_p is slightly different. Furthermore, the Q_{ave} of embedded SFTHX is higher than that of the welded SFTHX for f_p of 2.5 and 3.2 mm; however, the Q_{ave} is reversed for a f_p of 4.2 mm. Fig. 2(b) presents the relationship between h_o and V_{fr}. For welded SFTHXs, the h_o increases with increasing f_p. When f_p increases from 2.5 mm to 4.2 mm, h_o increases by approximately 17–28% for $f_p =$ 4.2 mm and 7–10% for $f_p = 3.2$ mm. For the welded SFTHX, the effect of f_p on h_o is negligible. Under the same experimental conditions, the h_o of the welded SFTHX is higher than that of the embedded SFTHX by up to 57%. The welded SFTHX had an additional characteristic at the fin base connection. The metal slags at the fin base lead to flow turbulence, which results in increased convective heat transfer. For Fig. 2(c), the ΔP increases with decreasing f_p because, when f_p decreases, the blockage of the heat exchanger's flow area increases. At the same fin pitch and experimental conditions, the pressure drop of the welded SFTHX is higher than that of the embedded SFTHX by approximately 26–28%. The ΔP for $f_p = 2.5$ mm is higher than that for $f_p = 3.2$ mm by approximately 8–12% for embedded SFTHX and 20–37% for welded SFTHX, as well as approximately 19–25% higher for embedded SFTHX and 37–57% higher for welded SFTHX when $f_p = 4.2$ mm.

Fig. 3 illustrates the ASP in terms of j and f factors at various Re_{do}, m_w, and $T_{w,in}$. The results demonstrate that the j and f factors decrease as Re_{do} increases. As seen in Fig. 3(a), (b), and 3(c), the variations of m_w (0.167–0.233 kg/s) and $T_{w,in}$ (55–65 °C) have negligible effects on the j and f for embedded and welded SFTHXs. The effect of f_p, is clearly seen; the f_p has no significant effect on the j factor for the embedded SFTHX. Nevertheless, the j factor for the welded SFTHX increases with increasing fin pitch. When f_p increases from 2.5 to 3.2 and 4.2 mm, the j factor for the welded SFTHX increases by approximately 9–10% for $f_p = 3.2$ mm and 14–26% for $f_p =$ 4.2 mm under the Re_{do} range of 4,000–16,000. Moreover, f_p has a significant effect on the f for both fin types. The results show that f_p increases as the f factor increases. The f factor for $f_p = 2.5$ mm is lower than that for $f_p = 3.2$ mm by approximately 11–18% for the embedded SFTHX and 16–26% for the welded SFTHX. In addition, for $f_p = 4.2$ mm, the f factor is lower by 35–47% for the embedded SFTHX and 30–35% for the welded SFTHX. These results can be easily explained by Eq. (8). The A_o, $A_{\min}$, and G_c (i.e., the air mass flux calculated from the minimum free flow area), which relate to f_p, are included in this equation. As a result, those parameters have a significant influence upon the f factor, specifically when $A_{\min}/A_o$ increases due to an increase in f_p, which leads to a higher f factor. For the effect of the fin base connection, the welded SFTHX has a higher f than the embedded SFTHX does at the same fin pitch. Both fin types exhibit similar f trends. In general, the difference range between the f factor for each fin pitch at various Re_{do} is 26–52%.

For implementation and future research, the dimensionless terms (i.e., j and f factors) modified from Pongsoi et al. [10] ($j = aRe_{do}^{b}$ and $f = aRe_{do}^{b}$) are proposed for the heat exchanger design and other applications. The fin pitch is included in the dimensionless terms

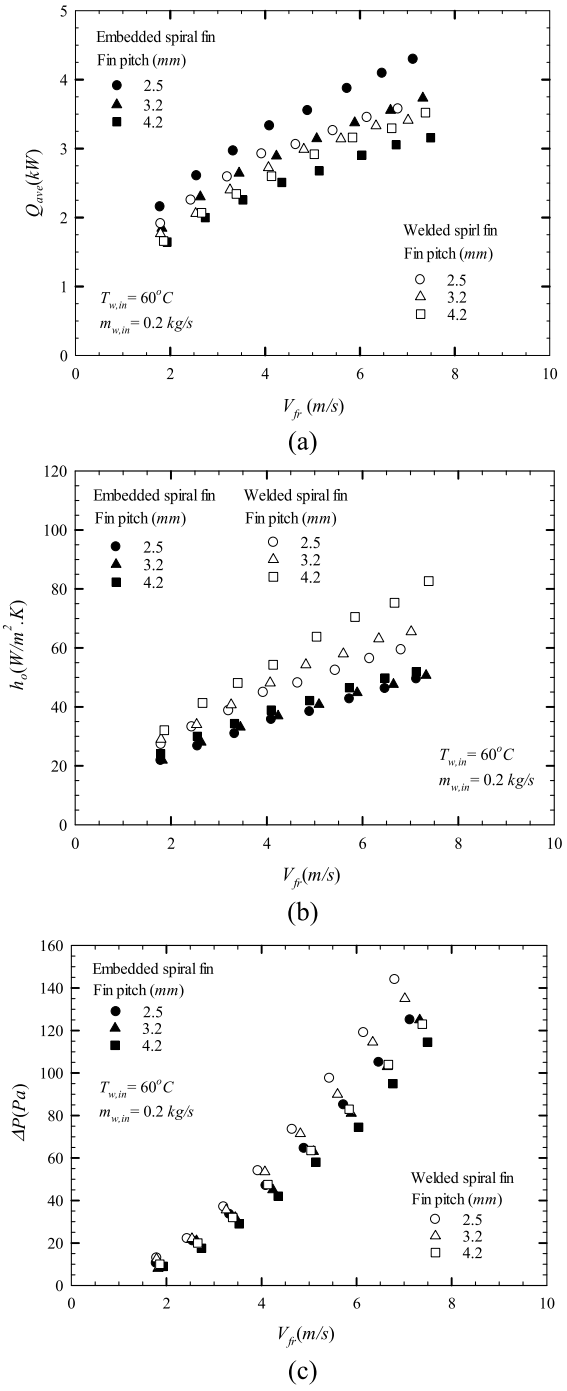

Fig. 2. Influence of fin base connection and fin pitch on the (a) Q_{ave}, (b) h_o, and (c) ΔP of embedded SFTHXs and welded SFTHXs (f_p = 2.5, 3.2, and 4.2 mm).

as the ratio of fin pitch and outside tube diameter (f_p/d_o). The new correlations for j and f of embedded and welded SFTHXs are proposed as follows.

For embedded SFTHX,

$$j_{em} = 0.1569 Re_{do}^{-0.3952} \tag{9}$$

$$f_{em} = 1.0402 Re_{do}^{-0.1724} \left(\frac{f_p}{d_o}\right)^{0.7116} \tag{10}$$

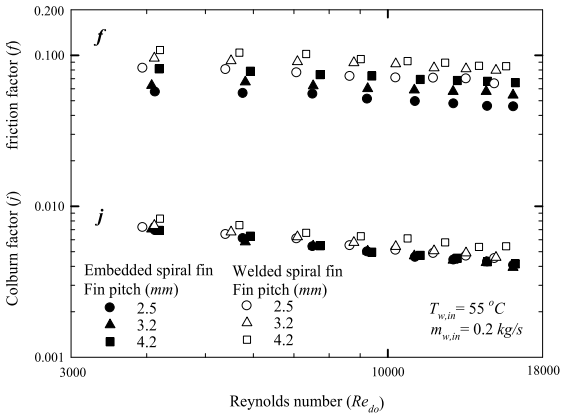

Fig. 3. Influence of the fin base and fin pitch on the *j* and *f* factors at (a) $m_{w,in} = 0.2$ kg/s, $T_{w,in} = 55$ °C, (b) $m_{w,in} = 0.2$ kg/s, $T_{w,in} = 60$ °C and (c) $m_{w,in} = 0.233$ kg/s, $T_{w,in} = 60$ °C.

For welded SFTHX,

$$j_{weld} = 0.3373 Re_{do}^{-0.3646} \left(\frac{f_p}{d_o}\right)^{0.3467} \tag{11}$$

$$f_{weld} = 1.1338 Re_{do}^{-0.1853} \left(\frac{f_p}{d_o}\right)^{0.4471} \tag{12}$$

Figs. 4 and 5 show that 100% of the measured data falls within ±10% of the proposed correlations. The mean deviations of *j* and *f*

correlations are 2.7 and 1.9% for the embedded SFTHX, respectively, and 3.2 and 3.3% for the welded SFTHX, respectively.

As shown in Fig. 6, the experimental data for embedded and welded SFTHXs are compared with results obtained from correlations of several fin types: plain fin (Wang and Chang [20] and Wang et al. [21]), circular fin (Briggs and Young [22] and Robinson and Briggs [23]), crimped spiral fin (Pongsoi et al. [3]), L-footed spiral fin (Pongsoi et al. [7]), and serrated spiral fin (Pongsoi et al. [10]). The plots show comparisons between the present data points and previous correlations in terms of *j* and *f* factors. As shown in Fig. 6(a), the results show that the embedded and welded SFTHX data have similar trends and values, as obtained from the correlations of the plain

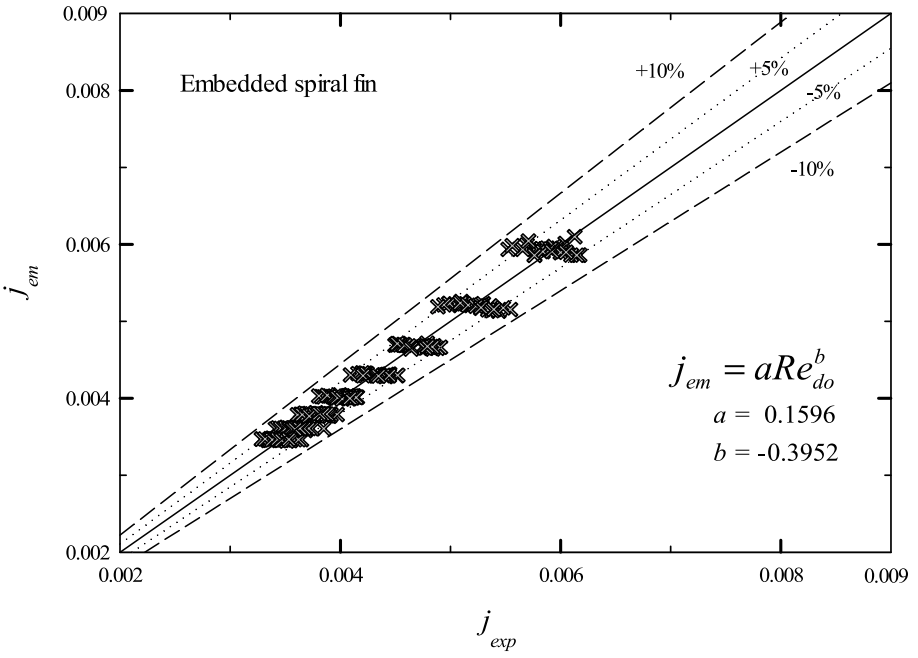

(a)

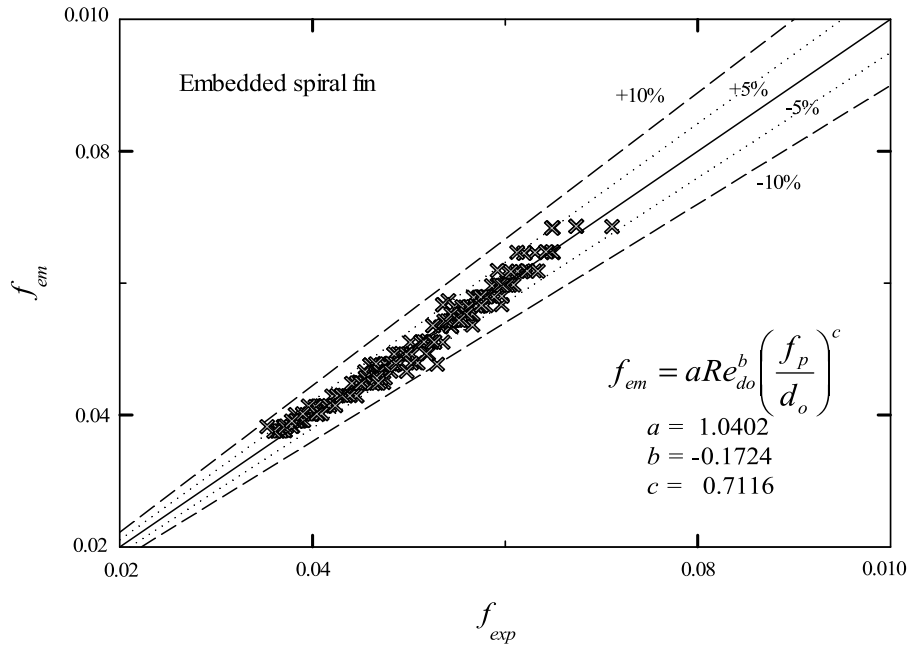

(b)

Fig. 4. The measured data vs. present correlations for the embedded SFTHX's (a) Colburn factor and (b) friction factor.

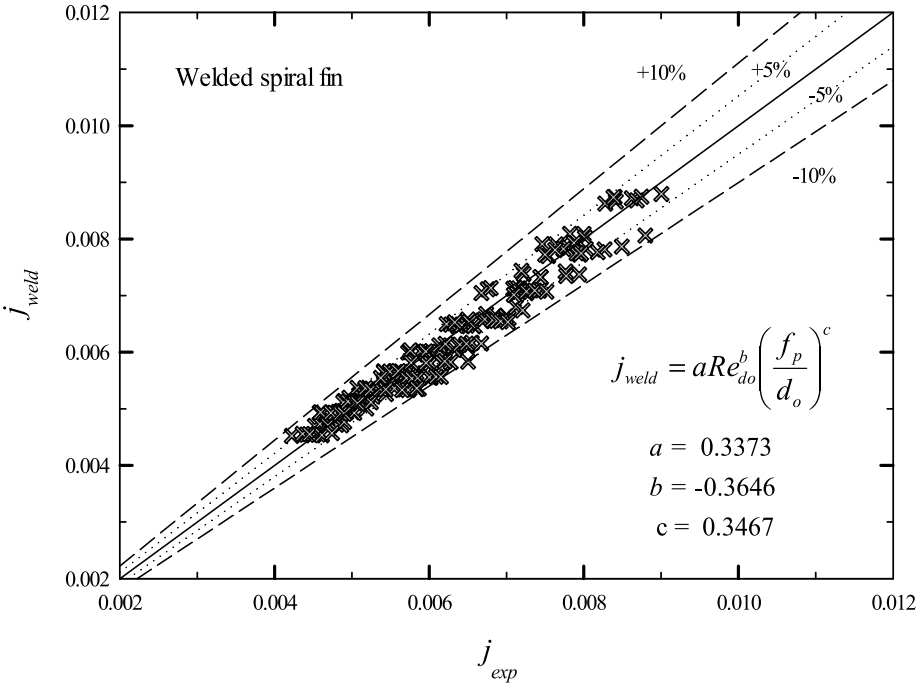

(a)

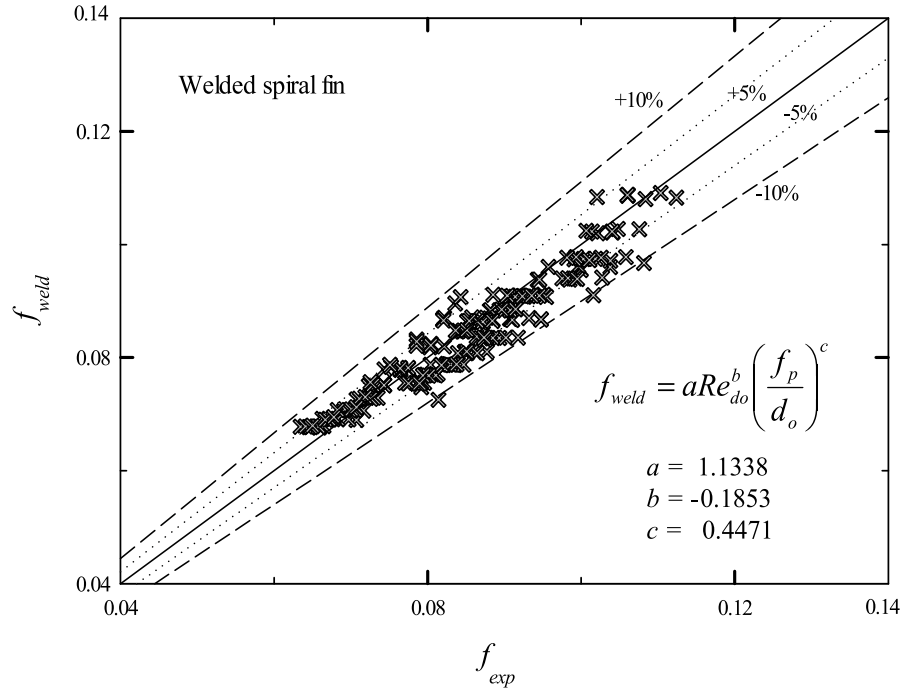

(b)

Fig. 5. The measured data vs. present correlations for the welded SFTHX's (a) Colburn factor and (b) friction factor.

fin, circular fin, and L-footed spiral fin. The embedded and welded SFTHXs have significantly different heat-transfer performances, when compared with the crimped spiral fin and the serrated spiral fin, due to the differences in fin patterns. For Fig. 6(b), the *f* factors of embedded and welded SFTHXs are higher than those for the circular fin, crimped spiral fin, and L-footed spiral fin are. In contrast,

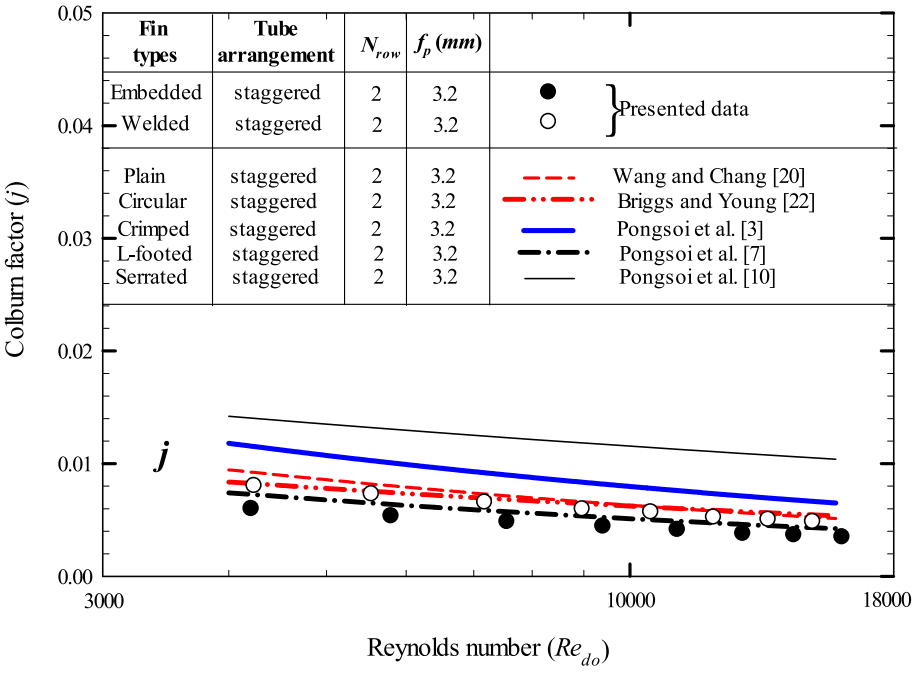

(a)

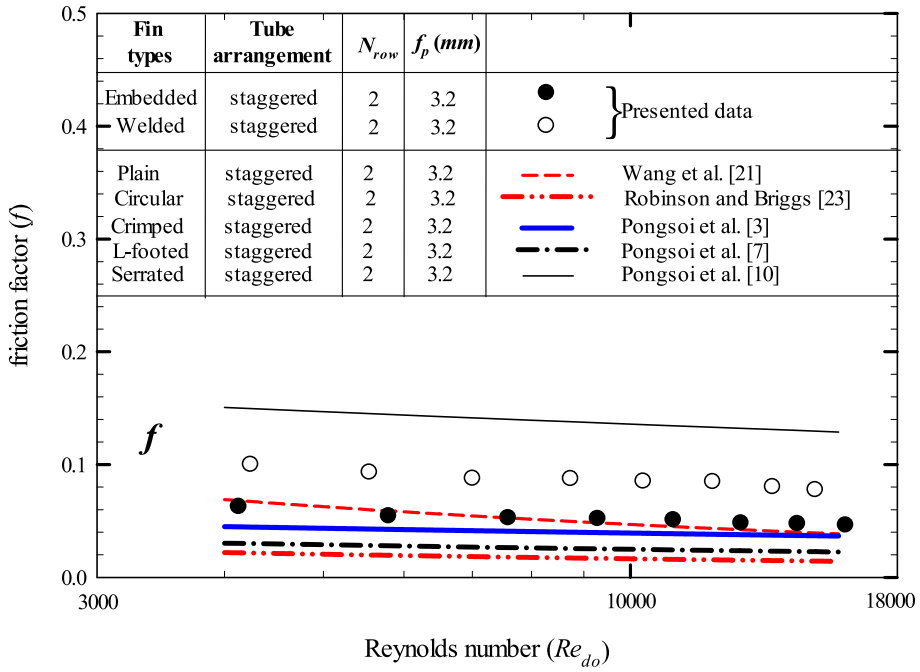

(b)

Fig. 6. The measured data vs. several correlations for (a) j factor and (b) f factor.

the f factor for the embedded and welded SFTHXs is lower than that for the serrated spiral fin.

4. Conclusion

The effect of f_p and fin base connections on the ASPs of embedded and welded SFTHXs under sensible heating conditions at high Re_{do} were investigated. The f_p measurements were 2.5–4.2 mm, whereas the fin base connections included embedded and welded finned tubes. The experiment is summarized as follows:

- The f_p and fin base connection have important roles in the ASPs of embedded and welded SFTHXs at high Re_{do}.
- The Q_{ave} and ΔP decreased with increasing f_p for embedded and welded SFTHXs.
- The h_o of the welded SFTHX increased when the f_p increased. However, the f_p had no significant effect on h_o for the embedded SFTHX.
- The f_p increased as the f factor increased for embedded and welded SFTHXs, but the j factor of the embedded SFTHX decreased less when compared with the welded SFTHX.
- The j and f correlations are proposed for predicting the heat exchanger's ASP.

CRediT author statement

Parinya Kiatpachai: Investigation (experimental), Data curation, Writing-Original draft, Writing-reviewing and editing. **Thawatchai Kaewkamrop**: Investigation (experimental), **Mehrdad Mesgarpour**: Investigation (experimental), Data curation. **Ho Seon Ahn, Ahmet Selim Dalkılıç, Omid Mahian**: Investigation (experimental). **Somchai Wongwises**: Supervision, Writing-reviewing and editing.

Declaration of competing interest

The authors declare that they have no known competing financial interests or personal relationships that could have appeared to influence the work reported in this paper.

Acknowledgments

The work was supported by the "Research Chair Grant" National Science and Technology Development Agency (NSTDA), Thailand and the Thailand Science Research and Innovation (TSRI), Thailand under Fundamental Fund 2022 (Project: Advanced Materials and Manufacturing for Applications in New S-curve Industries).

References

[1] P. Pongsoi, S. Pikulkajorn, S. Wongwises, Heat transfer and flow characteristics of spiral fin-and- tube heat exchangers: a review, International Journal of Heat and Mass Transfer 79 (2014) 417–431.
[2] P. Pongsoi, Pikulkajorn, S. Wongwises, Effect of fin pitches on the air-side performance of crimped spiral fin-and-tube heat exchangers with a multipass parallel and counter cross-flow configuration, Int. Journal of Heat and Mass Transfer 54 (2011) 2234–2240.
[3] P. Pongsoi, S. Pikulkajorn, C.C. Wang, S. Wongwises, Effect of number of tube rows on the air- side performance of crimped spiral fin-and-tube heat exchangers with a multipass parallel and counter cross-flow configuration, Int. Journal of Heat and Mass Transfer 55 (2012) 1403–1411.
[4] P. Pongsoi, S. Pikulkajorn, S. Wongwises, Effect of fin pitches on the optimum heat transfer performance of crimped spiral fin-and-tube heat exchangers, International Journal of Heat and Mass Transfer 55 (2012) 6555–6566.
[5] T. Keawkamrop, L.G. Asirvatham, A.S. Dalkılıç, H.S. Ahn, O. Mahian, S. Wongwises, An experimental investigation of the air-side performance of crimped spiral fin-and-tube heat exchangers with a small tube diameter, International Journal of Heat and Mass Transfer 178 (2021), 121571.
[6] P. Pongsoi, S. Pikulkajorn, S. Wongwises, Experimental study on the air-side performance of a multipass parallel and counter cross-flow L-footed spiral finand-tube heat exchanger, Heat Transfer Eng 33 (15) (2012) 1–13.
[7] P. Pongsoi, P. Promoppatum, S. Pikulkajorn, S. Wongwises, Effect of fin pitches on the air-side performance of L-footed spiral fin-and-tube heat exchangers, Int. Journal of Heat and Mass Transfer 59 (2013) 75–82.
[8] A. Ramesh, M.J.A. Prasanth, A. Kirthivasan, M. Suresh, Heat transfer studies on air cooled spiral radiator with circumferential fins, Procedia Engineering 127 (2015) 333–339.
[9] S. Unger, M. Beyer, J. Thiele, U. Hampel, Experimental study of the natural convection heat transfer performance for finned oval tubes at different tube tilt angles, Experimental Thermal and Fluid Science 105 (2019) 100–108.
[10] P. Pongsoi, S. Pikulkajorn, S. Wongwises, Air-side performance of serrated welded spiral fin-and- tube heat exchangers, International Journal of Heat and Mass Transfer 89 (2015) 724–732.
[11] H. Zhou, D. Liu, Q. Sheng, M. Hu, Y. Cheng, K. Cen, Research on gas side performance of staggered fin-tube bundles with different serrated fin geometries, International Journal of Heat and Mass Transfer 152 (2020), 119509.
[12] W. Youssef, Y.T. Ge, S.A. Tassou, CFD modelling development and experimental validation of a phase change material (PCM) heat exchanger with spiral-wired tubes, Energy Conversion and Management 157 (2018) 498–510.
[13] A. Kumar, J.B. Joshi, A.K. Nayak, A comparison of thermal-hydraulic performance of various fin patterns using 3D CFD simulations, International Journal of Heat and Mass Transfer 109 (2017) 336–356.
[14] M. Bosnjakovic, S. Muhic, A. Cikic, Experimental testing of the heat exchanger with star-shaped fins international, Journal of Heat and Mass Transfer 149 (2020), 119190.
[15] S.M.A. Naqvi, Q. Wang, Performance enhancement of shell–tube heat exchanger by clamping anti-vibration baffles with porous media involvement, Heat Transfer Engineering 41 (2020) 1–16.
[16] S.W. Chang, P.-S. Wu, B.S. Wei, Aerothermal Performance Improvement by Array of Pin-Fins with Spiral Wings, vol. 170, 2021, 107148.
[17] K.A. Gardner, Efficient of extended surface, ASME Trans 67 (1945) 621.
[18] W.M. Kays, A. London, Compact Heat Exchangers, third ed., Mcgraw-Hill, New York, 1984.
[19] ANSI/ASHRAE Standard 33-2000, Method of Testing Forced Circulation Air Cooling and Air Heating Coils, 2000.
[20] C.C. Wang, C.T. Chang, Heat and mass transfer for plate fin-and-tube heat exchangers with and without hydrophilic coating, International Journal of Heat and Mass Transfer 41 (1998) 3109–3120.

[21] C.C. Wang, Y.J. Chang, Y.C. Hsieh, Y.T. Lin, Sensible heat and friction characteristics of plate fin-and-tube heat exchangers having plane fins, International Journal of Refrigeration 19 (4) (1996) 223–230.
[22] D.E. Briggs, E.H. Young, Convective heat transfer and pressure drop of air flowing across triangular pitch banks of finned tubes, Chemical Engineering Progress Symposium Series 59 (41) (1963) 1–10.
[23] K.K. Robinson, D.E. Briggs, Pressure drop of air flowing across triangular pitch banks of finned tubes, AlChE Chemical Engineering Progress Symposium Series 62 (64) (1966) 177–184.